electronics

MDPI

Article

Linear Antenna Array Pattern Synthesis Using Multi-Verse Optimization Algorithm

Anoop Raghuvanshi [1,2], Abhinav Sharma [1,*], Abhishek Kumar Awasthi [3], Rahul Singhal [1], Abhishek Sharma [4], Sew Sun Tiang [5], Chin Hong Wong [6,7] and Wei Hong Lim [5,*]

1 Department of Electrical and Electronics Engineering, University of Petroleum and Energy Studies, Dehradun 248007, India; anoop@birlainstitute.co.in (A.R.); rahul.singhal@ddn.upes.ac.in (R.S.)
2 Department of ECE, Birla Institute of Applied Sciences, Bhimtal 263136, India
3 Paras Antidrone Technologies Private Limited, Navi Mumbai 400706, India; abhishekawasthi@parasantidrone.com
4 Department of Computer Science and Engineering, Graphic Era Deemed to be University, Dehradun 248002, India; abhisheksharma.cse@geu.ac.in
5 Faculty of Engineering, Technology and Built Environment, UCSI University, Kuala Lumpur 56000, Malaysia; tiangss@ucsiuniversity.edu.my
6 Maynooth International Engineering College, Maynooth University, W23 A3HY Maynooth, Ireland; chinhong.wong@mu.ie
7 Maynooth International Engineering College, Fuzhou University, Fuzhou 350116, China
* Correspondence: abhinav.sharma@ddn.upes.ac.in (A.S.); limwh@ucsiuniversity.edu.my (W.H.L.)

Abstract: The design of an effective antenna array is a major challenge encountered in most communication systems. A much-needed requirement is obtaining a directional and high-gain radiation pattern. This study deals with the design of a linear antenna array that radiates with reduced peak-side lobe levels (PSLL), decreases side-lobe average power with and without the first null beamwidth (FNBW) constraint, places deep nulls in the desired direction, and minimizes the close-in-side lobe levels (CSLL). The nature-inspired metaheuristic algorithm multi-verse optimization (MVO) is explored with other state-of-the-art algorithms to optimize the parameters of the antenna array. MVO is a global search method that is less prone to being stuck in the local optimal solution, providing a better alternative for beam-pattern synthesis. Eleven design examples have been demonstrated, which optimizes the amplitude and position of antenna array elements. The simulation results illustrate that MVO outperforms other algorithms in all the design examples and greatly enhances the radiation characteristics, thus promoting industrial innovation in antenna array design. In addition, the MVO algorithm's performance was validated using the Wilcoxon non-parametric test.

Keywords: linear antenna array; pattern synthesis; metaheuristic; MVO; PSLL; CSLL; side lobe average power; FNBW; Wilcoxon

Citation: Raghuvanshi, A.; Sharma, A.; Awasthi, A.K.; Singhal, R.; Sharma, A.; Tiang, S.S.; Wong, C.H.; Lim, W.H. Linear Antenna Array Pattern Synthesis Using Multi-Verse Optimization Algorithm. *Electronics* **2024**, *13*, 3356. https://doi.org/10.3390/electronics13173356

Academic Editors: Yiming Liu, Zhi Zhang and Yue Meng

Received: 2 July 2024
Revised: 19 August 2024
Accepted: 21 August 2024
Published: 23 August 2024

1. Introduction

The antenna has a significant impact on any communication system. Specifically, it is required that the antenna has sufficient gain and high directivity for effective communication between the transmitter and receiver end. To attain this, the single-element antenna requires considerable adjustment. Hence, a better option is to use an antenna array [1–3]. An array of antennas is used to enhance the signal-to-interference plus noise ratio (SINR), boost overall gain, provide beam control, cancel out interference, measure the direction of the arrival of incoming signals [4], and play a vital role in next-generation communication systems. Antenna array elements can be arranged in different ways, i.e., linear, circular, planar, and concentric rings [5]. Moreover, in modern wireless communication systems, reflect array, transmit array, metasurface, and conformal array antennas play a significant role in achieving desired radiation characteristics. Conformal array antennas [6,7] are designed to conform to specific shapes and are helpful in aerodynamics and healthcare

applications. The reflect array antenna consists of reflecting elements that can electronically steer the beam in the desired direction. Metasurface antennas utilize engineering surfaces with sub-wavelength structures, which can be useful in the Internet of Things (IoT) and fifth-generation communication systems. However, due to the simplicity of design and the numerous benefits of linear antenna arrays in several military and commercial applications, this research is focused on linear antenna arrays [8–11].

The procedure to ascertain the parameters of the antenna array to acquire desired radiation characteristics is referred to as pattern synthesis. Antenna array synthesis aims to create an array's physical layout with a radiation pattern that closely resembles the intended pattern [12,13]. Over the last two decades, researchers have proposed several methods to optimize the parameters of antenna arrays to obtain desired radiation characteristics [14–17]. The goal of the most common synthesis technique is to reduce the SLL while maintaining the main beam's gain [18]. However, the research is also concentrated towards overcoming the impact of interference and jamming signals [19]. The spacing and amplitude of the antenna elements can be optimized to retain the main beam's gain and suppress the SLL for different antenna geometries [20].

Generally, the antenna array has many radiating elements. Therefore, there is always a possibility that one or more of the elements fails [10]. The SLL is increased when an antenna element fails, destroying the antenna array's symmetry and perhaps disrupting the field strength throughout the array. It is not feasible to replace the faulty array element in certain circumstances, such as in a space station or on a battlefield. Nonetheless, it is feasible that the radiation pattern of an antenna array is retained using pattern synthesis with minimum quality deterioration and avoiding the need to replace the defective element [21,22].

Although SLL reduction, null positioning, and narrow beamwidth are desired radiation characteristics, the coupling effect between the antenna elements must be considered as it affects the antenna array's performance. In [23], the author proposed a robust beam-pattern-synthesis method that combines the compensation method with a constraint on magnitude response to mitigate the mutual coupling effect. In [24], the authors proposed a novel strategy where the refinement of joint-element rotation/phase optimization for pattern synthesis of linear and planar antenna arrays is outlined. However, conventional derivative-based techniques [25–28] are applied to solve such non-linear problems of the antenna design, but sometimes they are computationally complex and have a probability of getting trapped in a local optimum solution. Therefore, researchers have been motivated to explore metaheuristic algorithms [29–32] for pattern synthesis of different antenna array geometries over the last few years. In [33], the author explored fungi kingdom expansion for optimizing the radiation pattern of the antenna array and achieved a 100% success rate in different designs in comparison to other metaheuristic algorithms. In [34], the author utilized a social network optimization algorithm for the design of a shaped beam reflectarray and validated the optimized results through a full-wave approach. Moreover, these algorithms also find wide applications in radio frequency (RF) and microwave to enhance the system performance. In [35], the authors explored Bayesian optimization for setting the parameters of the power amplifiers, whereas in [36], the authors proposed a multi-objective digital predistortion technique for minimizing the RF power of power amplifiers. In [37], an efficient surrogate modelling and optimization technique was utilized for generating the efficient design of the microwave filters, whereas in [38], the author solved the multi-objective optimization problem of multi-layer microwave dielectric filters with the help of an artificial bee colony algorithm.

In this paper, the MVO algorithm [3] has been explored to optimize the current amplitude and interelement spacing between the array elements to attain a wide range of radiation characteristics. However, the MVO algorithm has not been utilized in linear antenna array-pattern synthesis to suppress the PSLL, minimize the side-lobe average power, and place deeper nulls in the desired direction while maintaining the FNBW and CSLL minimization.

The paper is structured as: Section 2 outlines the design equations of the linear antenna array. Section 3 highlights the mathematical layout of the nature-inspired MVO algorithm. Section 4 highlights the simulation results, and Section 5 provides closing remarks and avenues for future work.

2. Design Equation of a Linear Antenna Array

In this section, a linear antenna array with 2N isotropic elements is outlined and shown in Figure 1. The elements of the arrays are placed symmetrically with symmetry along the x-axis. The array factor of the antenna array in the azimuthal plane is mathematically defined as:

$$AF(\theta) = 2\sum_{n=1}^{N} I_n \cos\{kx_n \cos(\theta) + {}_n\} \quad (1)$$

where,

I_n: Excitation amplitude
$\varnothing_n$: Phase of nth element
x_n: Position of nth element in the array
k: $\frac{2\pi}{\lambda}$ is the wave number
θ: Azimuthal angle
λ: Wavelength

The equation of the array factor has three steering parameters, which may be adjusted to improve the antenna array's radiation pattern. These parameters are the current amplitude, position between the antenna elements and the phase of the excitation current.

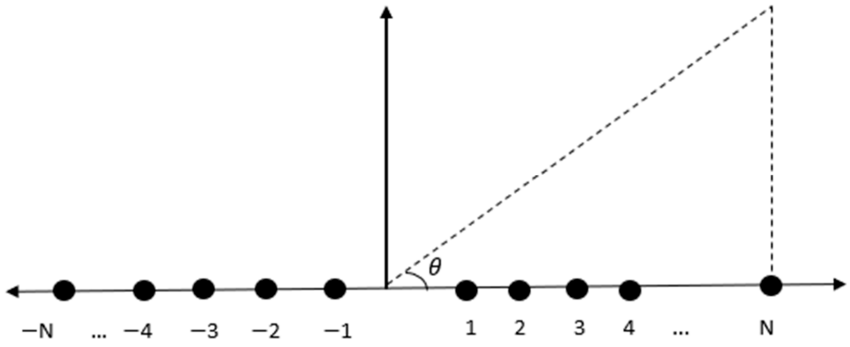

Figure 1. Linear antenna array with 2N number of elements placed along the x-axis.

In current amplitude optimization, the inter-element spacing between the antenna elements is kept as half the wavelength, i.e., $\lambda/2$, and the phase of the individual elements is zero, i.e., $\varnothing_n = 0$. Keeping these values, the array factor of Equation (1) is modified as:

$$AF(\theta) = 2\sum_{n=1}^{N} I_n \cos\{kx_n \cos(\theta)\}$$

$$AF(\theta) = 2\sum_{n=1}^{N} I_n \cos\left\{\frac{2\pi}{\lambda} \times \frac{\lambda}{2}\cos(\theta)\right\}$$

$$AF(\theta) = 2\sum_{n=1}^{N} I_n \cos\{\pi \times \cos(\theta)\} \quad (2)$$

In position optimization of the array elements, the elements must have constant amplitude and phase excitation, i.e., $I_n = 1$ and $\varnothing_n = 0$. Considering these values, the array factor of Equation (1) is changed as:

$$AF(\theta) = 2\sum_{n=1}^{N} \cos\{kx_n \cos(\theta)\} \quad (3)$$

Antenna element placement plays a significant role because the elements interelement spacing affects the antenna array's radiation pattern. Mutual coupling effects will occur while placing the elements too close, whereas grating lobes arise when the elements are positioned too far apart. Therefore, mutual coupling and grating lobes can be avoided if

the antenna elements are spaced apart with spacing lies between quarter wavelength and half wavelength, which can be mathematically stated as:

$$\frac{\lambda}{4} < |x_{n+1} - x_n| < \frac{\lambda}{2} \tag{4}$$

where x_n and x_{n+1} is the position of the nth and $(n + 1)$th antenna elements from the origin.

3. Multiverse Optimization Algorithm

The MVO algorithm is a population-based metaheuristic algorithm introduced by Mirjalili in 2014 and is inspired by the theories of cosmology. Multiverse is a popular theory of multiple universes where there is an interaction and possibly even collision between several entities of the universe such as white, black, and wormholes. The cyclic model of the multiverse theory postulates that collisions between parallel universes cause large bangs and white holes. Moreover, black holes act entirely differently from white holes, and their extraordinarily strong gravitational pull draws everything, even a beam of light. The holes that join disparate regions of a universe together are known as wormholes. According to the multiverse idea, wormholes function as time/space tunnels that allow items to travel between any two points in a universe immediately.

MVO algorithm is modelled on this stated concept where the entities are exchanged among the universe with the help of black and white hole tunnels and randomly between the universe through wormholes. White and black holes allow the algorithm to explore new solutions in the search space with local optima avoidance. In contrast, movement through the hole maintains a balance between the exploration and exploitation phases of the algorithm. The two adaptive parameters, wormhole existence probability (WEP), and travelling distance rate (TDR) emphasize exploitation and allow the algorithm to discover the optimal solution around the best solution. Thus, the MVO algorithm has few tuning parameters and, therefore, provides an appropriate balance to exploration and exploitation, especially in complex and high-dimensional space, in comparison to other optimization algorithms. The algorithm can also handle multiple objectives through weighted sum, Pareto front, or by incorporating constraints into the optimization problem. Moreover, the algorithm's performance is influenced by the number of variables, which can be maintained either by increasing the number of universes and iterations or by hybridizing the algorithm with other local search techniques. However, it increases the computational complexity of the algorithm. The flow chart of the MVO algorithm is presented in Figure 2.

The mathematical model of the MVO algorithm is outlined as follows:

Step 1: Initialize the population of universes (M) in the search space:

$$M = \begin{bmatrix} y_1^1 & y_1^2 & \cdots & y_1^o \\ y_2^1 & y_2^2 & \cdots & y_2^o \\ \vdots & \vdots & \vdots & \vdots \\ y_s^1 & y_s^2 & \cdots & y_s^o \end{bmatrix} \tag{5}$$

where o represents the number of parameters and s denotes the number of universes.

Step 2: Initialize WEP and TDR.

Step 3: Evaluate the fitness (inflation rate) of all the universe, normalize it, sort it based on their inflation rate, and identify the best universe.

Step 4: The universe exchange objects through white/black hole tunnel (exploration), and the white holes are selected through a roulette wheel mechanism, which is defined based on the following equation:

$$y_a^b = \begin{cases} y_l^b & rn1 < N(Ma) \\ y_a^b & rn1 \geq N(Ma) \end{cases} \tag{6}$$

where y_a^b is the bth parameter of the ath universe, Ma is the ath universe, $N(Ma)$ is the normalized rate of inflation of the ath universe, and $rn1$ is the any number between [0, 1], y_l^b is the bth parameter of the lth universe.

Step 5: The objects are transferred randomly without considering the inflation rate between a universe and the best universe through wormholes (exploitation) and are defined as:

$$y_a^b = \begin{cases} \begin{cases} Y_b + TDR \times ((u_b - l_b) \times rn4 + l_b) & rn3 < 1/2 \\ Y_b - TDR \times ((u_b - l_b) \times rn4 + l_b) & rn3 \geq 1/2 \end{cases} & rn2 < WEP \\ y_a^b & rn2 \geq WEP \end{cases} \quad (7)$$

where Y_b is the bth parameter of the best universe, l_b is the lower bound of the bth variable, u_b is the upper bound of the bth variable, y_a^b is the bth parameter of the ath universe, and $rn2$, $rn3$, $rn4$ are any numbers between [0, 1].

Step 6: Update WEP and TDR as follows:

$$WEP = min + l \times \left(\frac{max - min}{L} \right) \quad (8)$$

where min and max are the minimum and the maximum values, while l and L are the present iteration and the total number of iterations.

$$TDR = 1 - \frac{l^{1/p}}{L^{1/p}} \quad (9)$$

where p signifies the exploitation accuracy over the course of iterations.

Step 7: Reinitialize the universes that go beyond the search space.

Step 8: Go to Step 3 until the termination criteria are satisfied, which is either the total number of iterations or the minimum error between the two consecutive inflation rates.

Step 9: The best universe represents the global optimum solution.

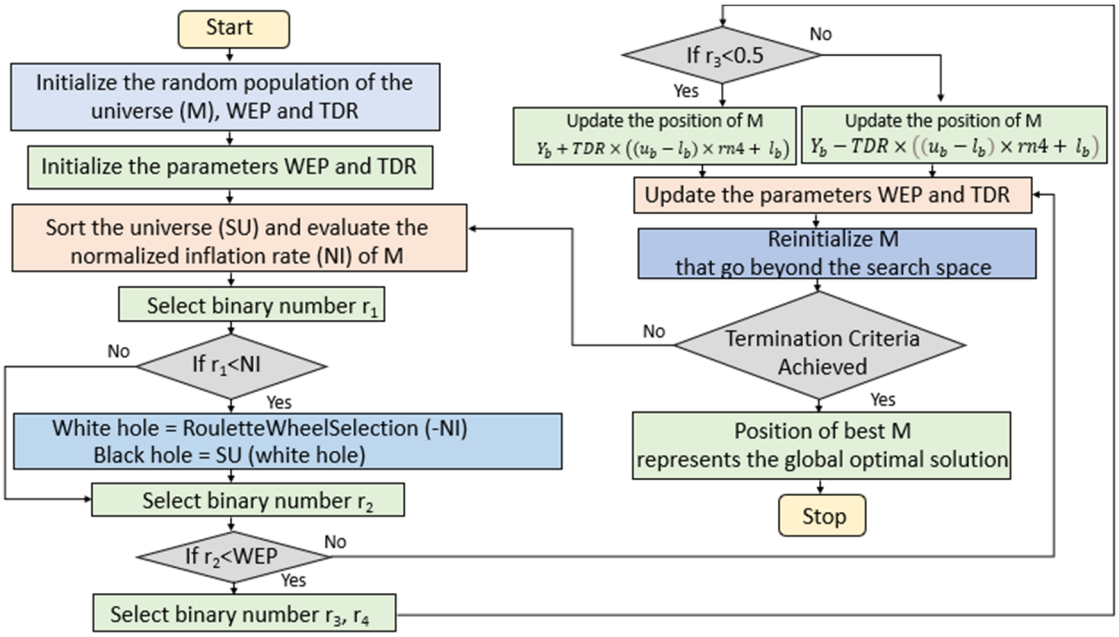

Figure 2. Flowchart of the multiverse-optimization algorithm.

4. Results and Discussion

This section discusses simulation results for the pattern synthesis of the linear antenna array using the MVO algorithm. The MVO algorithm is explored to estimate the antenna array elements' current amplitude and interelement spacing to achieve desired radiation characteristics. This research aims to minimize PSLL, reduce CSLL, and minimize side-lobe average power along with null placement in the desired direction with and without any constraint on beam width. To support this, 11 design examples are presented, of which six examples optimize the amplitude and five optimize the position of antenna elements.

The simulations are performed in MATLAB R2023a software on an i5 processor with 16 GB of RAM and are executed 15 times to obtain the optimum solution. MVO is a population-based iterative optimization algorithm. Therefore, 40 search agents are considered, which optimizes the solution under 1000 iterations. Design examples AA to AE demonstrate the optimization of the amplitude of antenna elements, while design example of PA to PE illustrates the optimization of the position of antenna elements using the MVO algorithm.

4.1. Excitation Current Amplitude Optimization

Excitation current amplitude (I_n) is the critical parameter in controlling the radiation characteristics of the phased array antennas. The amplitudes of the antenna array are optimized considering the uniform phase, i.e., $\varnothing_n = 0$, and uniform spacing, i.e., $\lambda/2$. The array factor of Equation (2) is modified with these two conditions and is considered for attaining all the desired objectives. Design examples AA, AB1, and AB2 optimize the current amplitudes of the antenna array for PSLL and side-lobe average power reduction, while AC minimizes the side lobes along with the placement of deep nulls in the intended direction. CSLL is minimized in the design example AD, and the side lobe's average power, along with the first null beamwidth constraint, is considered in the design example AE.

4.1.1. Peak Side-Lobe Level Minimization

The radiation pattern of an antenna has a desired main lobe and an undesired minor lobe, which exist in almost all antenna systems. One of the prime constraints in any antenna array design is that it radiates maximum power in its main lobe and less power in the side lobes. Therefore, the essential requirement of an antenna array is to suppress the peak side-lobe levels. The fitness function to achieve this objective is described in Equation (10), where θ represents the side-lobe region.

$$fitness = min\left[max\left(\frac{20log|AF(\theta)|}{max\ |AF(\theta)|}\right)\right] \tag{10}$$

The design example AA has $2N$ = 14 elements placed linearly where the side lobes are minimized in the region $\theta = [0°, 76°]$ and θ = [104°, 180°]. The fitness function is simulated by applying four different optimization algorithms: Ant Lion optimization (ALO), Dung Beetle algorithm (DBO), Whale optimization algorithm (WOA), and MVO algorithm for the sake of PSLL minimization. Table 1 shows the optimized values of the excitation current amplitudes for the right half side of the 14-element linear antenna array using different optimization algorithms, and Figures 3 and 4 present the array pattern in decibels (dB) against the azimuthal angle and the distribution of currents against the array elements. The MVO algorithm provides the PSLL of −38 dB, which is 24.84 dB down as compared to the uniform array, 12.12 dB down as compared to the ALO algorithm, and 17.58 dB down as compared to the DBO algorithm, which can also be observed in Table 2. For antenna array amplitude optimization, the computation time taken by respective ALO, DBO, WOA, and MVO algorithms is 13 s, 7.48 s, 11.75 s, and 7 s.

Table 1. Positive half-side values of optimized current amplitude for design example AA.

Method	Normalized Excitation Current Amplitudes						
ALO	1.0000	0.9476	0.8490	0.7158	0.5630	0.4070	0.4059
DBO	1.0000	0.9462	0.8447	0.7105	0.5557	0.4024	0.4024
WOA	1.0000	0.9452	0.8432	0.7072	0.5532	0.3982	0.3982
MVO	1.0000	0.9202	0.7758	0.5949	0.4066	0.2415	0.1342

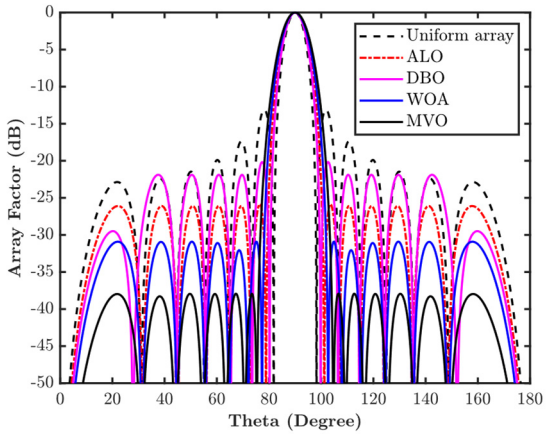

Figure 3. Array pattern of design example AA.

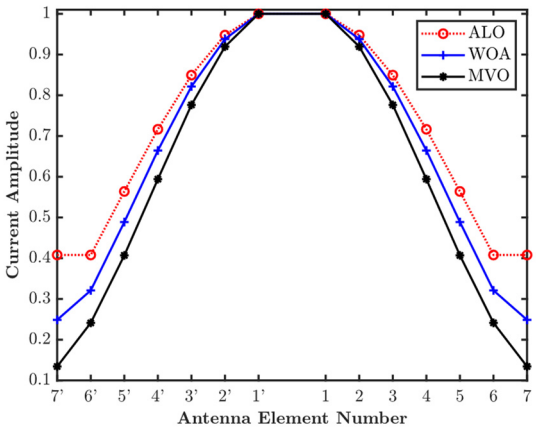

Figure 4. Distribution of currents in 14 element LAA of design example AA.

Table 2. Peak SLL for design example AA.

Method	Peak SLL (dB)
Uniform Array	−13.16
ALO	−25.88
DBO	−20.42
WOA	−30.94
MVO	−38.00

4.1.2. Side-Lobe Average-Power Minimization without FNBW Constraint

One of the choices is to suppress the total average power of the side lobes to enhance the power level of the main beam. For this, an objective that minimizes the side-lobe average power of a 20-element linear antenna array is presented in design examples AB1 and AB2. The fitness function formulated to meet this design objective of side-lobe average-power minimization is mathematically defined in Equation (11), where θ_{li} and θ_{ui} are the minimum and maximum limits of the region where the SLL is reduced and $\Delta\theta_i = [\theta_{ui} - \theta_{li}]$

is the difference between them. For the design example AB1, the values of the side lobes for one half of the antenna array are considered as $\theta_{li1} = 0^\circ$ and $\theta_{ui1} = 82^\circ$, and for the other half, the values are $\theta_{li2} = 98^\circ$ and $\theta_{ui2} = 180^\circ$.

$$fitness = \sum_i \frac{1}{\Delta\theta_i} \int_{\theta_{li}}^{\theta_{ui}} |AF(\theta)|^2 d\theta \tag{11}$$

The current amplitudes for design example AB1 are shown in Table 3, and the array pattern is presented in Figure 5. Compared to the other cutting-edge optimization algorithms, MVO obtains lower side lobes, and the average power of the side lobe region is minimized to a greater extent.

Table 3. Positive half-optimized current amplitudes for design example AB1.

Method	Optimized Excitation Current Amplitudes									
ALO	1.0000	0.9692	0.9145	0.8302	0.7410	0.6196	0.5217	0.3835	0.3376	0.3374
DBO	1.0000	0.9710	0.9137	0.8300	0.7353	0.6202	0.5086	0.3451	0.3451	0.3451
MVO	1.0000	0.9660	0.9038	0.8135	0.7095	0.5850	0.4722	0.3428	0.2637	0.2055

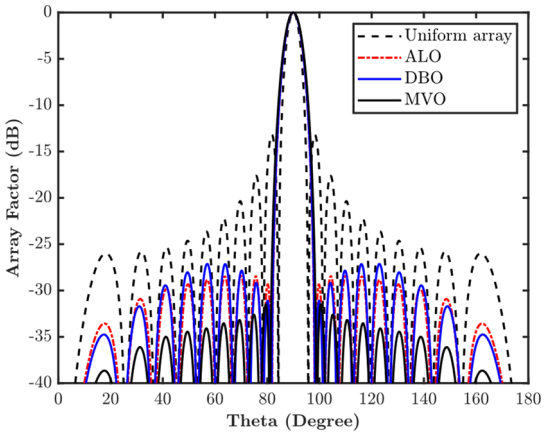

Figure 5. Array pattern for design example AB1.

The peak SLL of the uniform linear antenna array of design AB1 is at −13.18 dB, which is now reduced to −31.49 dB by using the MVO algorithm. Hence, there is a reduction of 18.51 dB in the first SLL, and similarly, in the other minor lobes, there is a significant reduction of side lobes by the MVO algorithm compared to ALO and DBO algorithms. This reduction in the side lobe levels of design AB1 is tabulated in Table 4. The amplitude of the antenna elements has a unity value at the center of the array, and it decreases as one reaches the edge of the array element for both halves of the 20-element linear antenna array.

Table 4. Positive half-side lobe levels of a 20-element LAA for design example AB1.

Method	Side Lobe Level (dB)								
Uniform array	−13.18	−17.76	−20.43	−22.54	−23.63	−24.84	−25.33	−25.77	−26.01
ALO	−29.33	−28.00	−28.00	−28.48	−29.04	−29.34	−29.85	−30.99	−33.56
DBO	−31.14	−29.16	−27.94	−27.14	−27.14	−28.08	−29.44	−31.75	−34.75
MVO	−31.49	−32.66	−33.17	−33.54	−34.11	−34.46	−35.01	−36.12	−38.65

The design example AB2 is presented for synthesizing a 32-element linear antenna array for side-lobe average-power minimization with amplitude optimization. For this design, the side lobes are placed at $\theta_{li1} = 0^\circ$, $\theta_{ui1} = 82^\circ$, $\theta_{li2} = 98^\circ$ and $\theta_{ui2} = 180^\circ$. The fitness function of Equation (11) is optimized using MVO and other algorithms. The fitness

function presented in Equation (11) has been considered for optimization using MVO and other algorithms. The obtained values of the optimized current amplitude are outlined in Table 5, based on how the array pattern is drawn and is shown in Figure 6. An MVO-optimized antenna array offers the highest reduction for all the side lobes compared to other applied algorithms, which is also shown in Table 6. Hence, the proposed MVO algorithm efficiently optimizes the current amplitude of the large size antenna arrays in comparison to other applied optimization algorithms.

Table 5. Positive half-optimized current amplitudes for design example AB2.

Method	Optimized Excitation Current Amplitudes							
ALO	0.5276	0.5588	0.6187	0.6944	0.7832	0.8636	0.9393	0.9767
	1.0000	0.9695	0.9257	0.8190	0.7335	0.5615	0.5183	0.5183
DBO	0.7382	0.7382	0.7382	0.7382	0.7382	0.8817	0.9614	0.9753
	1.0000	0.9661	0.9305	0.7382	0.7382	0.7382	0.7382	0.7382
WOA	0.6503	0.6784	0.7296	0.7914	0.8596	0.9175	0.9741	0.9915
	1.0000	0.9547	0.8967	0.7799	0.6918	0.5197	0.4501	0.4501
MVO	1.0000	0.9846	0.9557	0.9115	0.8565	0.7892	0.7159	0.6335
	0.5500	0.4636	0.3837	0.3016	0.2346	0.1654	0.1258	0.1001

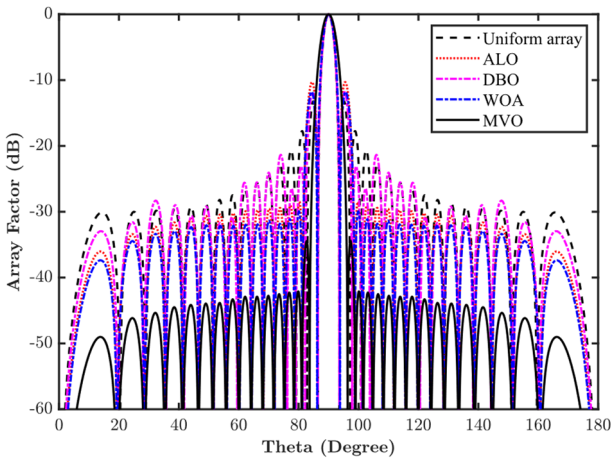

Figure 6. Array pattern for design example AB2.

Table 6. PSLL of a 32 element LAA for design example AB2.

Method	Side Lobe Level (dB)													
Uniform array	−13.48	−17.80	−20.78	−22.71	−24.32	−25.76	−26.79	−27.59	−28.20	−28.86	−29.29	−29.61	−29.88	−30.02	−30.09
ALO	−10.35	−28.50	−29.06	−29.42	−29.68	−29.82	−30.06	−30.22	−30.54	−30.69	−31.05	−31.71	−32.28	−33.43	−36.03
DBO	−11.85	−23.16	−26.55	−21.49	−24.19	−25.59	−25.64	−30.89	−31.71	−29.41	−30.81	−29.01	−28.33	−31.61	−32.96
WOA	−11.88	−30.09	−31.33	−31.83	−31.57	−31.97	−32.09	−32.30	−32.29	−32.25	−32.45	−33.00	−33.49	−34.45	−37.41
MVO	−34.63	−42.16	−42.46	−42.63	−42.80	−42.91	−42.90	−43.32	−43.92	−43.94	−44.22	−44.52	−45.38	−46.23	−49.02

4.1.3. Side-Lobe Average-Power Minimization, along with Null Placement

In many situations, side-lobe average-power minimization is required along with null positioning in the direction of the interfering sources. To incorporate this, a design example AC of a 20-element linear antenna array is formulated with the fitness function defined in Equation (12), where θ_k is the angle of the interfering source where the nulls have to be positioned. The side lobes for one-half of the antenna array are considered as $\theta_{li1} = 0^\circ$

and $\theta_{ui1} = 82°$. For the other half, these values are $\theta_{li2} = 98°$ and $\theta_{ui2} = 180°$. The nulls are intended at 64°, 76°, 104°, and 116°.

$$fitness = \sum_i \frac{1}{\Delta\theta_i} \int_{\theta_{li}}^{\theta_{ui}} |AF(\theta)|^2 d\theta + \sum_k |AF(\theta_k)|^2 \quad (12)$$

The array pattern obtained for design example AC is illustrated in Figure 7. It displays that the side-lobe average power obtained by the MVO algorithm has a minimum value compared to the ALO and DBO algorithms, and the desired deeper nulls were obtained. The side-lobe levels for the right half of the design AC are tabulated in Table 7. On average, a nearly 13.58 dB reduction was observed for the side-lobe average power with a maximum of 16.6 dB and a minimum of 10.2 dB. Table 8 presents the null depth of ALO, DBO, and MVO algorithms at 64°, 76°, 104°, and 116°. The simulation result shows that the MVO algorithm achieves minimum SLL and places deep nulls in the intended direction compared to the ALO and DBO algorithms.

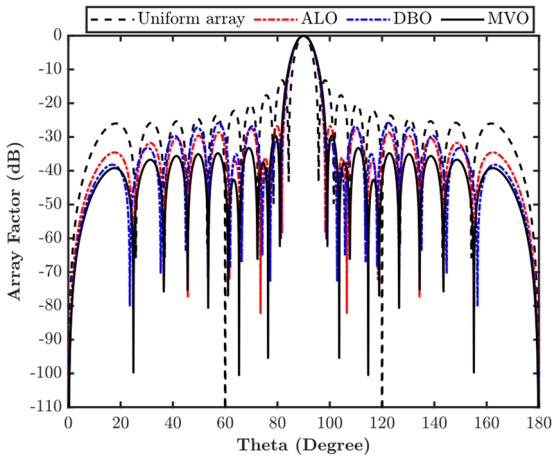

Figure 7. Array pattern for design example AC.

Table 7. Positive half-side lobe levels of a 20-element LAA for design example AC.

Method	Side-Lobe Level (dB)								
Uniform array	−13.18	−17.76	−20.43	−22.54	−23.63	−24.84	−25.33	−25.77	−26.01
ALO	−26.80	−36.18	−27.45	−37.38	−28.69	−29.56	−30.39	−31.81	−34.55
DBO	−30.72	−39.41	−26.83	−35.07	−25.82	−27.18	−29.57	33.26	−38.22
MVO	−29.78	−37.57	−33.27	−42.67	−34.81	−35.10	−35.62	−36.73	−39.21

Table 8. Null depth of a 20-element LAA for design example AC.

Required Nulls at	64°	76°	104°	116°
Method	**Null Depth (dB)**			
ALO	−66.90	−66.90	−66.90	−66.90
DBO	−67.30	−72.20	−72.20	−67.30
MVO	−100.50	−95.41	−95.41	−100.50

4.1.4. Close-In Side-Lobe Level Minimization

The close-in side lobe, i.e., the first lobe adjacent to the main lobe, is minimized by optimizing the fitness function formulated in Equation (13), where θ_{AS} is the total region of the side lobes and θ_{NS} is the region of close side lobes. α_1 and α_2 are the weights that add a greater degree of freedom on the level of side-lobe reduction. Design example AD presents 10 elements of a linear antenna array for close-in-side-lobe level reduction.

$$fitness = (\alpha_1 max\{20\log|AF(\theta_{AS})|\} + \alpha_2 max\{20\log|AF(\theta_{NS})|\}) \quad (13)$$

where θ_{AS} is considered as $[0°, 76°]$ and $[104°, 180°]$, while θ_{NS} is considered as $[69°, 76°]$ and $[104°, 111°]$. The optimum value of the weights α_1 and α_2 are 1 and 2, respectively.

The amplitude of the excitation current obtained by the MVO algorithm for one-half of the 10-element linear antenna array is outlined in Table 9.

Table 9. Positive half values of optimized excitation current amplitudes for design example AD.

Method	Optimized Excitation Current Amplitudes				
ALO	1.0000	0.6787	0.5111	0.5111	0.5111
DA	1.0000	0.6787	0.5111	0.5111	0.5111
MVO	1.0000	0.6788	0.5111	0.5111	0.5111

Figure 8 illustrates the array pattern of design example AD for close-in side-lobe level reduction. The simulation result shows that the CSLL of the uniform array is −12.97 dB and reduced to −30.19 dB using the MVO algorithm. Hence, a reduction of 17.22 dB is obtained in the design example AD.

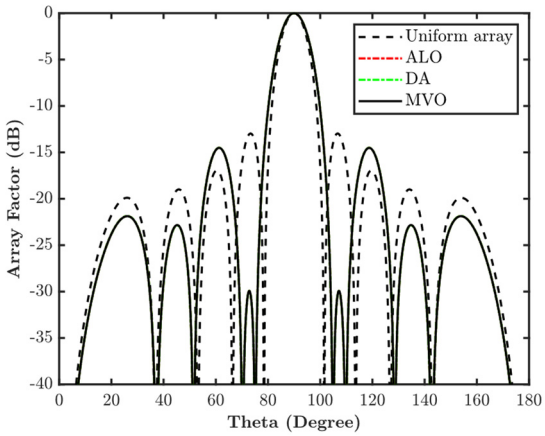

Figure 8. Array pattern for design example AD.

4.1.5. Side-Lobe Level Minimization with FNBW Constraint

An effective antenna array system should have a radiation pattern with minimum SLL and narrow beamwidth. However, both parameters are interrelated. Therefore, design example AE minimizes the side lobes with the constraint on the first null beamwidth. Since the main lobe is predominantly focused on the required signal, the null constraint is imposed to enhance the quality of the signal with a reduced noise level. Similarly, the system has better spatial resolution and can differentiate closely spaced sources. To achieve this objective, the fitness function of Equation (14) is optimized using the MVO algorithm. This design example is considered for a 20-element linear antenna array. The array pattern is shown in Figure 9, indicating that the average power of the side lobes is reduced while the beamwidth remains constant using the MVO algorithm compared to ALO and WOA. However, the beamwidth tolerance of ±5% is considered in this design example. Table 10 presents the PSLL and FNBW of conventional, ALO, WOA, and MVO-optimized linear antenna arrays. The simulation results illustrate that MVO presents comparable results among other algorithms.

$$fitness = C_1 \times \sum_i \frac{1}{\Delta\theta_i} \int_{\theta_{li}}^{\theta_{ui}} |AF(\theta)|^2 d\theta + C_2 \times \left(FNBW_{Computed} - FNBW(I_n = 1) \right) \quad (14)$$

where C_1 and C_2 are the weighting coefficient, and FNBW represents the first null beamwidth. $FNBW_{Computed}$ is the computed FNBW, and $FNBW(I_n = 1)$ is the FNBW for uniform excitation current ($I_n = 1$) and uniform inter-element distance between the elements.

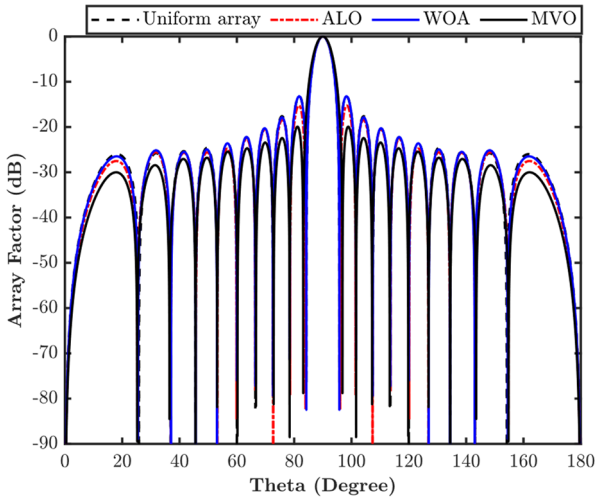

Figure 9. Array pattern for design example AE.

Table 10. PSLL and FNBW for design example AE.

Method	PSLL (dB)	FNBW (Degree)
ULA	−13.22	11.48
ALO	−15.28	12.10
SWOA	−13.29	11.50
MVO	−20.00	13.70

4.2. Element-Position Optimization

The interelement spacing or position of the antenna elements alters the directional characteristic of the antenna system. It decides the side-lobe levels, null placement, and the antenna array's return loss. Therefore, the position is considered one of the prime parameters for improving radiation characteristics. This section presents five antenna design examples PA to PE for position optimization of the array element for PSLL minimization, side-lobe average-power minimization with and without null placement, CSLL minimization, and side-lobe reduction with the first null beamwidth constraint.

The positions (x_n) of the array elements are optimized considering the uniform current amplitudes $I_n = 1$ and phase $\varnothing_n = 0$. The array factor used to achieve this objective is outlined in Equation (3).

4.2.1. Peak-Side Lobe-Level Minimization

In the design example PA, peak-side lobe levels are minimized by optimizing the position of the 10-element linear antenna array. The fitness function formulated for this design example is presented in Equation (10). This design focuses on suppressing the level of the side lobes in the region $\theta = [0^\circ, 76^\circ]$ and $\theta = [104^\circ, 180^\circ]$.

Table 11 shows the position of array elements obtained using the MVO algorithm, and Figure 10 depicts their array patterns. The simulation's outcome illustrates that the PSLL is decreased to −22.03 dB using the MVO algorithm, which is 9.07 dB less than the peak value of the uniform linear antenna array and is presented in Table 12.

Table 11. Positive half values of optimized positions for design example PA.

Method	Optimized Element Positions				
ALO	0.2431 λ	0.3761 λ	0.8391 λ	1.1664 λ	1.7552 λ
BWOA	0.2049 λ	0.4078 λ	0.8285 λ	1.1692 λ	1.7498 λ
MVO	0.2416 λ	0.3774 λ	0.8387 λ	1.1667 λ	1.7552 λ

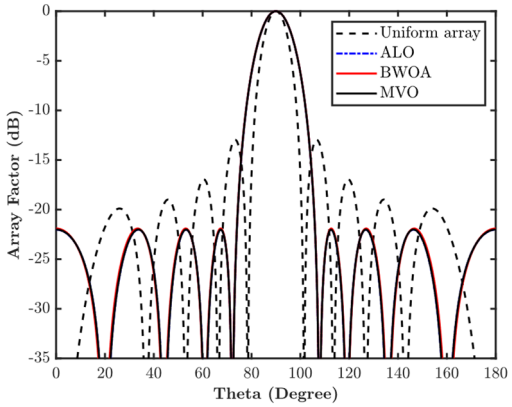

Figure 10. Array pattern for design example PA.

Table 12. Peak SLL for design example PA.

Method	Peak SLL (dB)
Uniform Array	−12.96
ALO	−22.03
BWOA	−21.90
MVO	−22.03

4.2.2. Side-Lobe Average-Power Minimization without FNBW Constraint

Design example PB optimizes the positions of a 20-element linear antenna array to minimize the average power of the side lobes. The fitness function formulated to meet this design objective is mentioned in Equation (11). In this design example, the side-lobe regions are considered as $\theta_{li1} = 0°$, $\theta_{ui1} = 82°$, $\theta_{li2} = 98°$, and $\theta_{ui2} = 180°$. The array pattern obtained for this design is shown in Figure 11, which is optimized using the DA and MVO algorithms. Table 13 summarizes the values of the side lobes, and around 6.13 dB of the average power is minimized with a highest difference of 9.25 dB and a lowest difference of 4.23 dB.

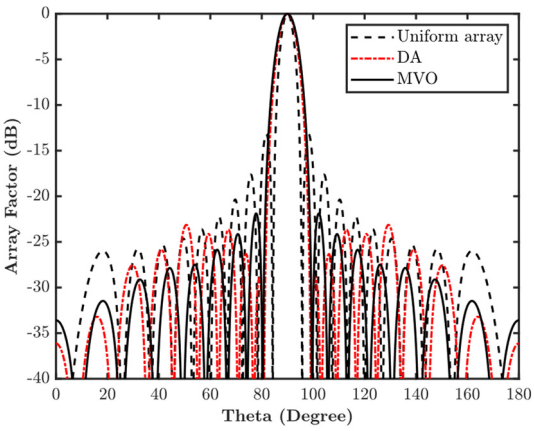

Figure 11. Array pattern for design example PB.

Table 13. Positive half-side lobe levels for design example PB.

Method	Side-Lobe Level (dB)							
Uniform array	−13.18	−17.76	−20.43	−22.54	−23.63	−24.84	−25.33	−25.77
DA	−29.00	−26.32	−23.66	−24.14	−23.15	−25.90	−27.58	−33.23
MVO	−22.43	−24.22	−25.86	−27.90	−27.86	−29.15	−31.49	−33.66

4.2.3. Side-Lobe Average-Power Minimization along with Null Placement

The side-lobe average-power reduction, along with the null placement of a 20-element linear antenna array, is presented in design example PC. The fitness function for this multi-objective function is mentioned in Equation (12), and the side-lobe region is $\theta_{li1} = 0°$, $\theta_{ui1} = 82°$, $\theta_{li2} = 98°$, and $\theta_{ui2} = 180°$. The direction of the required nulls is 64°, 76°, 104°, and 116°. Figure 12 presents the array pattern obtained by optimizing the separation of array elements depicted in Table 14 using the dragonfly algorithm (DA), black widow optimization algorithm (BWOA), and MVO algorithm. Tables 15 and 16 present the side lobe levels and null depth obtained using all three optimization algorithms. On average, the highest power reduction is attained using the MVO algorithm, along with the placement of deep nulls in the intended directions. Null depth of −70 dB and −78.11 dB is effectively achieved by the MVO algorithm, which is better than the DA and BWOA algorithm. DA provides the comparative null depth in comparison to the MVO algorithm at two null directions, but MVO presents an overall consistent null depth at all four locations.

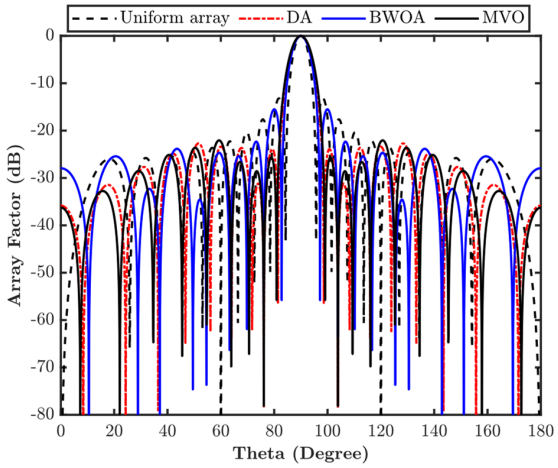

Figure 12. Array pattern for design example PC.

Table 14. Positive half values of optimized positions for design example PC.

Method	Optimized Element Positions									
DA	0.1981 λ	0.4491 λ	0.8871 λ	1.0608 λ	1.7637 λ	1.5673 λ	2.6363 λ	2.2811 λ	3.3262 λ	4.0654 λ
BWOA	0.1914 λ	0.5624 λ	1.0050 λ	1.4021 λ	1.7423 λ	2.2011 λ	2.5647 λ	3.0549 λ	3.5021 λ	4.1257 λ
MVO	0.2450 λ	0.4220 λ	0.6867 λ	1.2885 λ	1.2363 λ	1.8103 λ	3.2044 λ	2.1556 λ	2.5591 λ	3.9534 λ

Table 15. Positive half-side lobe levels for design example PC.

Method	Side-Lobe Level (dB)								
Uniform array	−13.18	−17.76	−20.43	−22.54	−23.63	−24.84	−25.33	−25.77	−26.01
DA	−23.88	−31.22	−23.65	−23.37	−22.71	−24.87	−27.68	−31.46	−35.92
BWOA	−15.51	−22.37	−25.53	−24.67	−34.55	−23.90	−32.29	−25.43	−27.98
MVO	−25.69	−28.64	−26.72	−22.06	−23.61	−25.14	−28.52	−32.74	−36.28

Table 16. Null depth for design example PC.

Required Nulls at	64°	76°	104°	116°
Method	**Null Depth (dB)**			
DA	−63.88	−78.48	−78.48	−63.88
BWOA	−66.33	−63.57	−63.57	−66.33
MVO	−70.00	−78.11	−78.11	−70.00

4.2.4. Close-In Side-Lobe Level Minimization

Design example PD considers a 10-element linear antenna array to optimize the position of the elements for reducing the level of the adjacent side lobes. The fitness function for this design example is outlined in Equation (13). Table 17 presents the optimized location of array elements obtained using the MVO algorithm, and Figure 13 shows the array pattern. The simulation's outcome shows that the CSLL is reduced to −45.79 dB by the MVO algorithm. Hence, it presents a suppression of 32.82 dB.

Table 17. Positive half values of optimized positions for design example PD.

Method	Optimized Element Positions				
ALO	0.2335 λ	0.3781 λ	0.8873 λ	1.4405 λ	2.1128 λ
MVO	0.1747 λ	0.4199 λ	0.8252 λ	1.4921 λ	2.0605 λ

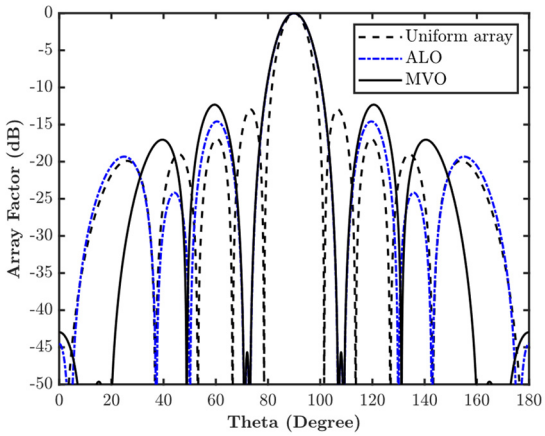

Figure 13. Array pattern for design example PD.

4.2.5. Side-Lobe Level Minimization with FNBW Constraint

Design example PE presents a 20-element linear antenna array for optimizing the position of antenna elements to suppress the average side-lobe power, while the beamwidth remains unchanged. The fitness function of Equation (14) is optimized using DA, DBO, BWOA, and MVO algorithms, and the optimized positions are presented in Table 18. Figure 14 shows the array pattern of this design, and the result depicts that the SLL is reduced while the beamwidth remains unchanged. Table 19 presents the PSLL and FNBW of conventional, DA, DBO, BWOA, and MVO algorithms for the linear antenna array. The simulation outcome illustrates that MVO presents comparable results among other algorithms.

Table 18. Positive half values of optimized positions for design example PE.

Method	Optimized Element Positions									
DA	0.2365 λ	0.7500 λ	1.2500 λ	1.7500 λ	2.2500 λ	2.7500 λ	3.2202 λ	3.7500 λ	4.2500 λ	4.7500 λ
DBO	0.2439 λ	0.7500 λ	1.2500 λ	1.7500 λ	2.2500 λ	2.7500 λ	3.2364 λ	3.7500 λ	4.2157 λ	4.7500 λ
BWOA	0.2456 λ	0.7500 λ	1.2500 λ	1.7500 λ	2.2500 λ	2.7500 λ	3.2500 λ	3.7500 λ	4.2079 λ	4.7500 λ
MVO	0.2427 λ	0.7496 λ	1.2493 λ	1.7500 λ	2.2473 λ	2.7500 λ	3.2402 λ	3.7500 λ	4.2161 λ	4.7500 λ

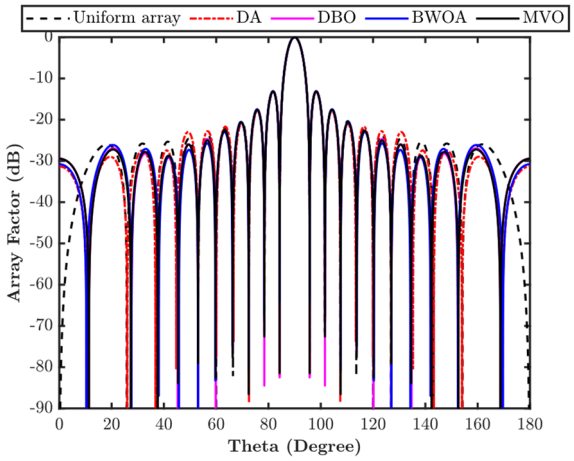

Figure 14. Array pattern for design example PE.

Table 19. PSLL and FNBW for design example PE.

Method	PSLL	FNBW
Uniform Array	−13.20	11.40
DA	−13.25	11.60
DBO	−13.15	11.50
BWOA	−13.12	11.40
MVO	−13.21	11.60

4.3. Validation of Results Using Full-Wave Approach

The full-wave analysis of two design examples AA and PA has been conducted in the EM-simulator CST microwave studio. A half-wavelength wire dipole is used as the radiator, and the optimized current amplitude of Table 1 was obtained using different optimization algorithms for a 14-element array and has been considered for obtaining the radiation pattern. Similarly, for design example PA 10, the element linear array with uniform excitation and optimized position of antenna element outlined in Table 11 has been utilized to obtain desired radiation characteristics. The simulation results suggest that there is a very close agreement between the results obtained using the full-wave approach, and the results were obtained using MATLAB software. Figures 15 and 16 show the array pattern of design example AA and PA were obtained using the full-wave approach.

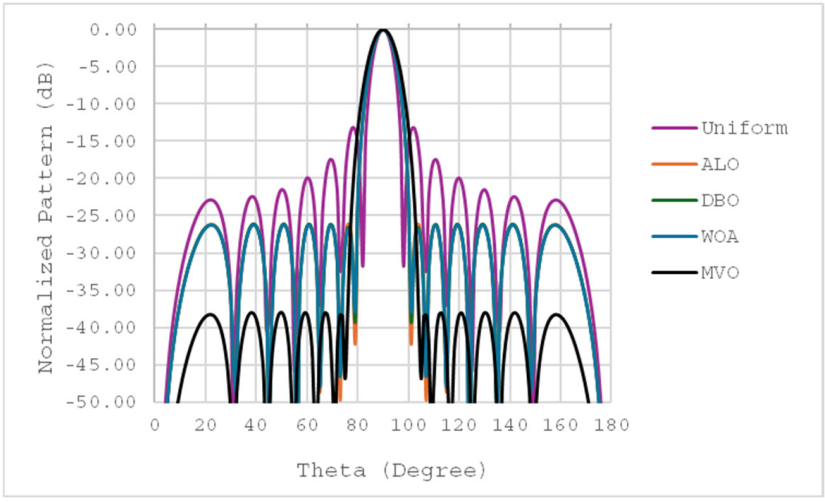

Figure 15. Array pattern of design example AA obtained using full-wave approach.

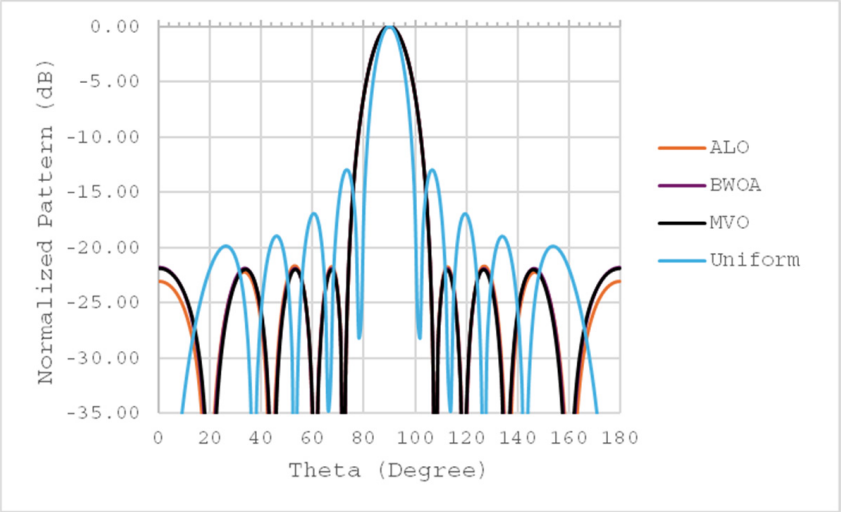

Figure 16. Array pattern of design example PA obtained using full-wave approach.

4.4. Statistical Validation

This section deals with the statistical evaluation of the MVO algorithm for all 11 design examples. The Wilcoxon rank-sum test is applied to analyze the robustness of the MVO algorithm over other applied metaheuristic optimization algorithms for 15 independent run values. The significance level for the rank sum test is 5%. The amplitude and position optimization test results of all the design examples are summarized in Tables 20 and 21. The result shows that the MVO algorithm continuously produces greater R^+ values than R^- values for all the antenna array-pattern synthesis design examples. Thus, the proposed MVO algorithm consistently outperforms other cutting-edge metaheuristic optimization algorithms (ALO, DA, DBO, WOA, and BWOA) that are explored for antenna array-pattern synthesis. This demonstrates the great potential of the suggested algorithm as a valid and effective tool for dealing with the difficulties associated with antenna array-pattern generation.

Table 20. Wilcoxon rank-sum test for all the design examples of amplitude optimization.

Design Example	Algorithm	R^+	R^-	Result
AA	MVO vs. ALO	742	258	+
	MVO vs. DBO	646	354	+
	MVO vs. WOA	742	258	+
AB1	MVO vs. ALO	851	149	+
	MVO vs. DBO	533	467	+
AB2	MVO vs. ALO	868	132	+
	MVO vs. DBO	808	192	+
	MVO vs. WOA	867	133	+
AC	MVO vs. ALO	751	249	+
	MVO vs. DBO	751	249	+
AD	MVO vs. ALO	979	21	+
	MVO vs. WOA	930	70	+
AE	MVO vs. ALO	999	1	+
	MVO vs. DA	966	34	+

Table 21. Wilcoxon rank-sum test for all the design examples of position optimization.

Design Example	Algorithm	R^+	R^-	Result
PA	MVO vs. ALO	999	1	+
	MVO vs. BWOA	964	36	+

Table 21. *Cont.*

Design Example	Algorithm	R^+	R^-	Result
PB	MVO vs. DA	661	339	+
PC	MVO vs. DA	901	99	+
	MVO vs. BWOA	659	341	+
PD	MVO vs. DA	717	283	+
	MVO vs. DBO	990	10	+
	MVO vs. BWOA	953	47	+
PE	MVO vs. ALO	950	50	+

5. Conclusions

This paper explores the MVO algorithm for improving the far-field radiation characteristics of the linear antenna array. The MVO algorithm has a good exploration and exploitation capability and has few tuning parameters. Therefore, it is an ideal choice for solving complex optimization problems of electromagnetic and antenna communities. In the first section of the paper, the MVO algorithm is explored in design examples AA-AE for optimizing the amplitudes of the antenna array for suppressing the PSLL and reducing the side-lobe average power with and without the first null beamwidth constraint while positioning the deep nulls in the intended directions and decreases the CSLL. The simulation results illustrate that in amplitude optimization in the 14-element array, the PSLL is minimized by 24.84 dB compared to the uniform linear array and outperforms other optimization algorithms. Similarly, side-lobe average power is minimized in 20- and 32-element arrays, and deep nulls -100.5 dB, -95.41 dB, -95.41 dB, and -100.5 dB are placed at 64°, 76°, 104°, and 116°. The CSLL is decreased in a 10-element array by 17.22 dB in comparison to a uniform linear array, and the side-lobe average power is minimized in a 20-element array while maintaining the FNBW with a tolerance of $\pm 5\%$.

In the second section, the interelement spacing between the antenna elements is optimized in design examples PA-PE using the MVO algorithm to achieve desired radiation characteristics. The simulation result shows that in a 10-element array, PSLL is reduced by 9.07 dB in comparison to the uniform linear array. The side-lobe average power is minimized for a 20-element linear antenna array with the placement of deep nulls -70 dB, -78.11 dB, -78.11 dB, and -70.00 dB at 64°, 76°, 104°, and 116°. In the design example PD for a 10-element array, the CSLL was suppressed by 32.82 dB. In the design example PE for a 20-element array, the side lobe average power is minimized while maintaining the FNBW at a tolerance of $\pm 5\%$.

The optimized values of amplitude and position for design examples AA and PA obtained using optimization algorithms have also been validated by the full-wave approach, and it is found that there is a very close proximity between the MATLAB and EM simulation results. The performance of the MVO algorithm for all the design examples is also analyzed using the Wilcoxon rank test over 15 independent runs. The result demonstrates that the MVO algorithm excels over all other algorithms and is suitable for antenna array-pattern synthesis. As a scope of future work, the MVO algorithm can be explored for the pattern synthesis of complex array geometries such as planar arrays, volumetric arrays, concentric circular arrays, and conformal arrays.

Author Contributions: Conceptualization, A.R., A.S. (Abhinav Sharma), R.S. and S.S.T.; Methodology, A.S. (Abhinav Sharma), A.S. (Abhishek Sharma), A.K.A. and C.H.W.; simulation, A.R., A.S. (Abhishek Sharma) and W.H.L.; writing—original draft, A.R., A.S. (Abhinav Sharma) and A.K.A.; writing—review and editing, A.R., A.S. (Abhinav Sharma), A.S. (Abhishek Sharma) and C.H.W.; visualization, R.S., A.K.A., S.S.T. and A.S. (Abhinav Sharma); supervision, A.S. (Abhinav Sharma) and A.K.A. All authors have read and agreed to the published version of the manuscript.

Funding: The study was funded by the Malaysian Ministry of Higher Education through the Fundamental Research Grant Scheme (FRGS/1/2024/TK07/UCSI/02/1) and UCSI University Research through the Excellence & Innovation Grant (REIG-FETBE-2022/038).

Data Availability Statement: Data are contained within the article.

Conflicts of Interest: Author Abhishek Kumar Awasthi was employed by the company Paras Antidrone Technologies Private Limited. The remaining authors declare that the research was conducted in the absence of any commercial or financial relationships that could be construed as a potential conflict of interest.

References

1. Teruel, O.G.; Iglesias, E.R. Ant colony optimization in thinned array synthesis with minimum sidelobe level. *IEEE Antennas Wirel. Propag. Lett.* **2006**, *5*, 349–352. [CrossRef]
2. Sharma, A. Antenna array pattern synthesis using metaheuristic algorithm: A review. *IETE Tech. Rev.* **2022**, *40*, 90–115. [CrossRef]
3. Mirjalili, S.; Mirjalili, S.M.; Hatamlou, A. Multi-verse optimizer: A nature-inspired algorithm for global optimization. *Neural Comput. Appl.* **2016**, *27*, 495–513. [CrossRef]
4. Sharma, A.; Mathur, S. Performance analysis of adaptive array signal processing algorithms. *IETE Tech. Rev.* **2016**, *33*, 472–491. [CrossRef]
5. Saxena, P.; Kothari, A. Ant lion optimization algorithm to control side lobe level and null depths in linear antenna arrays. *AEU-Int. J. Electron. Commun.* **2016**, *70*, 1339–1349. [CrossRef]
6. Beccaria, M.; Pirinoli, P.; Yang, F. Preliminary results on conformal transmitarray antennas. In Proceedings of the 2018 IEEE International Symposium on Antennas and Propagation & USNC/URSI National Radio Science Meeting, Boston, MA, USA, 8–13 July 2018; pp. 265–266.
7. Liu, Z.Q.; Zhang, Y.S.; Qian, Z.; Han, Z.P.; Ni, W. A novel broad beamwidth conformal antenna on unmanned aerial vehicle. *IEEE Antennas Wirel. Propag. Lett.* **2012**, *11*, 196–199. [CrossRef]
8. Pavani, T.; Padmavathi, K.; Kumari, C.U.; Ushasree, A. Design of array antennas via atom search optimization. *Mater. Today Proc.* **2023**, *80*, 2051–2054. [CrossRef]
9. Grewal, N.S.; Rattan, M.; Patterh, M.S. A linear antenna array failure correction using improved bat algorithm. *Int. J. RF Microw. Comput.-Aided Eng.* **2017**, *27*, 7.
10. Das, A.; Mandal, D.; Ghoshal, S.; Kar, R. An efficient side lobe reduction technique considering mutual coupling effect in linear array antenna using bat algorithm. *Swarm Evol. Comput.* **2017**, *35*, 26–40. [CrossRef]
11. Wang, A.; Li, X.; Xu, Y. BA-based low-PSLL beampattern synthesis in the presence of array errors. *IEEE Access* **2022**, *10*, 9371–9379. [CrossRef]
12. Almagboul, M.; Shu, F.; Qian, Y.; Zhou, X.; Wang, J.; Hu, J. Atom search optimization algorithm based hybrid antenna array receive beamforming to control sidelobe level and steering the null. *AEU-Int. J. Electron. Commun.* **2019**, *111*, 152854. [CrossRef]
13. Liu, L.; Wang, A.; Sun, G.; Zheng, T.; Yu, C. An improved biogeography-based optimization approach for beam pattern optimizations of linear and circular antenna arrays. *Int. J. Numer. Model. Electron. Netw. Devices Fields* **2021**, *34*, e2910. [CrossRef]
14. Han, L.; Yanheng, L.; Sun, G.; Wang, A.; Liang, S. Beam pattern synthesis based on improved biogeography-based optimization for reducing sidelobe level. *Comput. Electr. Eng.* **2017**, *60*, 161–174.
15. Guney, K.; Onay, M. Bees algorithm for interference suppression of linear antenna arrays by controlling the phase-only and both the amplitude and phase. *Expert Syst. Appl.* **2010**, *37*, 3129–3135. [CrossRef]
16. Li, X.; Yin, M. Optimal synthesis of linear antenna array with composite differential evolution algorithm. *Sci. Iran.* **2012**, *19*, 1780–1787. [CrossRef]
17. Zhang, R.; Zhang, Y.; Sun, J.; Li, Q. Pattern synthesis of linear antenna array using improved differential evolution algorithm with sps framework. *Sensors* **2020**, *20*, 5158. [CrossRef]
18. Rao, A.P.; Sarma, N. Synthesis of reconfigurable antenna array using differential evolution algorithm. *IETE J. Res.* **2017**, *63*, 428–434. [CrossRef]
19. Chakravarthy, V.; Chowdary, P.; Panda, G.; Anguera, J.; Andlijar, A.; Majhi, B. On the linear antenna array synthesis techniques for sum and difference patterns using flower pollination algorithm. *Arab. J. Sci. Eng.* **2018**, *43*, 3965–3977. [CrossRef]
20. Ram, G.; Panduro, M.A.; Reyna, A.; Kar, R.; Mandal, D. Pattern synthesis and broad nulling optimization of STMLAA with EM simulation. *Int. J. Numer. Model. Electron. Netw. Devices Fields* **2018**, *31*, e2322. [CrossRef]
21. Saxena, P.; Kothari, A. Linear antenna array optimization using flower pollination algorithm. *SpringerPlus* **2016**, *5*, 306. [CrossRef]
22. Zhao, K.; Liu, Y.; Hu, K. Optimal pattern synthesis of linear array antennas using the nonlinear chaotic grey wolf algorithm. *Electronics* **2023**, *12*, 4087. [CrossRef]
23. Zhang, T.; Ser, W. Robust beampattern synthesis for antenna arrays with mutual coupling effect. *IEEE Trans. Antennas Propag.* **2011**, *59*, 2889–2895. [CrossRef]
24. Liu, Y.; Li, M.; Haupt, R.L.; Guo, Y.J. Synthesizing shaped power patterns for linear and planar antenna arrays including mutual coupling by refined joint rotation/phase optimization. *IEEE Trans. Antennas Propag.* **2020**, *68*, 4648–4657. [CrossRef]

25. Zeng, S.; Yang, X.; Li, C.; Zhao, F. Fast descent search algorithm for shaped-beam synthesis with the desired field phases as design variables. *IEEE Trans. Antennas Propag.* **2023**, *71*, 3070–3079. [CrossRef]
26. Wang, Z.; Sun, G.; Tong, J.; Ji, Y. Pattern synthesis for sparse linear arrays via atomic norm minimization. *IEEE Antennas Wirel. Propag. Lett.* **2021**, *20*, 2215–2219. [CrossRef]
27. Hua, D.; Li, W.T.; Shi, X.W. Pattern synthesis for large planar antenna arrays using a modified alternating projection method. *Prog. Electromagn. Res.* **2014**, *37*, 149–160. [CrossRef]
28. Wang, Y.; He, X.; Wang, J.; Berezin, S.; Mathis, W. Antenna array pattern synthesis via coordinate descent method. *J. Electromagn. Anal. Appl.* **2015**, *7*, 168–177. [CrossRef]
29. Akdagli, A.A.; Guney, K.; Karaboga, D. Touring ant colony optimization algorithm for shaped-beam pattern synthesis of linear antenna. *Electromagnetics* **2006**, *26*, 615–628. [CrossRef]
30. Bera, R.; Cheruvu, S.; Kundu, K.; Upadhyay, P.; Mandal, D. Array antenna pattern synthesis using improved particle swarm optimization (IPSO) algorithm. *ECTI Trans. Electr. Eng. Electron. Commun.* **2023**, *21*, 249806. [CrossRef]
31. Subhashini, K.R.; Satapathy, J.K. Development of an enhanced ant lion optimization algorithm and its application in antenna array synthesis. *Appl. Soft Comput.* **2017**, *59*, 153–173. [CrossRef]
32. Saxena, P.; Kothari, A. Optimal pattern synthesis of linear antenna array using grey wolf optimization algorithm. *Int. J. Antennas Propag.* **2016**, *2016*, 1205970. [CrossRef]
33. Alnahwi, F.M.; Al-Yasir, Y.I.A.; Sattar, D.; Ali, R.S.; See, C.H.; Abd-Alhameed, R.A. A new optimization algorithm based on the fungi Kingdom expansion behavior for antenna applications. *Electronics* **2021**, *10*, 2057. [CrossRef]
34. Beccaria, M.; Niccolai, A.; Zich, R.E.; Pirinoli, P. Shaped-beam reflect array design by means of social network optimization (Sno). *Electronics* **2021**, *10*, 744. [CrossRef]
35. Mengozzi, M.; Gibiino, G.P.; Angelotti, A.M.; Santarelli, A.; Florian, C.; Colantonio, P. Automatic Optimization of Input Split and Bias Voltage in Digitally Controlled Dual-Input Doherty RF Pas. *Energies* **2022**, *15*, 4892. [CrossRef]
36. Mengozzi, M.; Gibiino, G.P.; Angelotti, A.M.; Florian, C.; Santarelli, A. GaN power amplifier digital predistortion by multi-objective optimization for maximum RF output power. *Electronics* **2021**, *10*, 244. [CrossRef]
37. Yu, Y.; Zhang, Z.; Cheng, Q.S.; Liu, B.; Wang, Y.; Guo, C.; Ye, T.T. State-of-the-Art: AI-Assisted Surrogate Modeling and Optimization for Microwave Filters. *IEEE Trans. Microw. Theory Tech.* **2022**, *70*, 4635–4651. [CrossRef]
38. Toktas, A. Multi-objective design of multilayer microwave dielectric filters using artificial bee colony algorithm. In *Nature-Inspired Metaheuristic Algorithms for Engineering Optimization Applications*; Springer: Singapore, 2021; pp. 357–372.